Lyman-alpha spectra from rotating outflows

Maria Camila Remolina-Gutiérrez[1] ⋆ & Jaime E. Forero-Romero [1] †

[1] *Departamento de Física, Universidad de los Andes, Cra. 1 No. 18A-10 Edificio Ip, CP 111711, Bogotá, Colombia*

3 November 2017

ABSTRACT
We perform Monte Carlo radiative transfer simulations of outflowing gas with additional solid body rotation. We reproduce the main features of the outcoming spectra with a simple semi-analytic model that modifies the spectra of outflows without rotation by adding a Doppler shift with the rotational information.

Key words: galaxies: dwarf — radiative transfer — Methods: numerical

1 INTRODUCTION

Distant galaxies are key to understand early evolutionary stages of our Universe. Physical conditions in those galaxies allow the emergence of a Lyman-α line emission at 1216 Å(Partridge & Peebles 1967). Galaxies detected through its Lyman-α emission receive the name of Lyman Alpha Emitters (LAEs).

Currently LAEs are commonly targeted in wide area galaxy surveys. They have been effectively used to study galaxy evolution, cosmology and the thermal history of the Universe. This has been possible through the study of their spatial distribution and the shape of their Lyα emission line.

Recent improvements in instrumentation have revolutionized the kind of studies that can be performed on LAEs. It is now possible to infer detailed kinematic maps for nearby galaxies. The study of these maps would allow us to build data-driven models to interpret the Lyα spectra of unresolved galaxies, helping us to constrain the physical conditions of the interstellar medium (ISM) processing the Lyα radiation.

One of the ISM's features that plays an important role in shaping the Lyα is HI kinematics. In a static HI medium the Lyα line ha two equal and symmetric peaks around the natural Lyα wavelength and zero intensity at the line's center. For an outflowing ISM, the line becomes asymmetrical with a more pronounced read peak. If the galaxy rotates, the line shows different amounts of Doppler shifts modifying the overall line profile (Garavito-Camargo et al. 2014).

In this paper we present for the first time a study of the joint effects of galaxy outflows and rotation. We study a simplified geometrical configuration corresponding to a spherical gas cloud with symmetrical radial outflows and a rotation profile corresponding to a solid body. We base our modeling on a Monte-Carlo radiative transfer code called CLARA

⋆ mc.remolina197@uniandes.edu.co
† je.forero@uniandes.edu.co

(Code for Lyman Alpha Radiation Analysis) presented for the first time by Forero-Romero et al. (2011). Besides modeling the impact of joint rotation and outflows, we also want to check to what extent the analytical model presented by Garavito-Camargo et al. (2014) to explain the effects of rotation can also be applied in our case.

In this paper we introduce first our theoretical tools and assumptions in Section 2. We continue in Section 3 with the results from the Monte-Carlo simulation, the comparison against the semi-analytical approximation which we use to make a thorough exploration of the effect of rotation. In Section 4 we discuss our results and their possible implications for observational analysis to finally present our conclusions in Section 5.

2 THEORETICAL MODELS

2.1 Monte-Carlo Radiative Transfer Model

CLARA follows the propagation of individual photons through a neutral Hydrogen medium characterized by its temperature, velocity field and global optical depth. The code assumes an homogeneous density throughout the simulated volume. In the current implementation we neglect the influence of dust. Our basic models is an spherical distribution of neutral hydrogen, an approximation commonly used in the literature, as it explains a wide variety of observational features (Ahn et al. 2003; Verhamme et al. 2006; Dijkstra et al. 2006).

The central element in this paper is the velocity field that captures outflows and rotation. Outflows are captured by a Hubble-like radial velocity profile with the velocity magnitude increasing linearly with the radial coordinate; the outflow model is fully characterized by V_{out}, the velocity at the sphere's surface. Rotation follows a solid body rotation profile, which is fully characterized by V_{rot}, the linear velocity at the sphere's surface.

The total velocity field corresponds to the superposition

$\tau_{\rm H}$	$v_{\rm rot}$ (km s^{-1})	$v_{\rm out}$ (km s^{-1})
10^5	{0}	{5, 25, 50}
10^6	{0}	{5, 25, 50}
10^7	{0}	{5, 25, 50}
10^5	{50, 100}	{25, 50, 75}
10^6	{50, 100}	{25, 50, 75}
10^7	{50, 100}	{25, 50, 75}

Table 1. Parameters' Values. List of values that were used to construct the radiative transfer models. Values in braces for a row indicate that all possible combinations in of $\tau_{\rm H}$, $v_{\rm rot}$ and $v_{\rm out}$ are used.

of rotation and outflows. The cartesian components take the following form:

$$v_x = \frac{x}{R}V_{\rm out} - \frac{y}{R}V_{\rm rot}, \tag{1}$$

$$v_y = \frac{y}{R}V_{\rm out} + \frac{x}{R}V_{\rm rot}, \tag{2}$$

$$v_z = \frac{z}{R}V_{\rm out}, \tag{3}$$

where x, y and z are the cartesian position coordinates with the origin at the sphere's center, R is the radius of the sphere and the direction of the angular velocity vector corresponds to the $\hat{k}$ unit vector.

For each model setup we follow 10^5 individual photons generated at the center of the sphere at the Lyα line's center as they propagate through the volume and finally scape. We store the final frequency and propagation direction for each photon at its last scattering.

In Table 1 we list the combination of $\tau_{\rm H}$, $v_{\rm rot}$ and $v_{\rm rot}$ values used in this paper. The range of values have some overlap with the expectations from a dwarf galaxy with a total neutral hydrogen mass of 10^8-10^9 $M_\odot$. We run a total of 24 different models.

2.2 Analytical Model for Bulk Rotation

Rotation induces two main effects on the Lyα line morphology. First. Break of spherical symmetry due to the preferential direction introduced by the rotation axis. This symmetry break is reflected in the observed spectra as a dependency on the viewing angle, θ, between the line of sight of a distant observer and the rotational velocity. Second. Line blurring as the rotational velocity increases. At a fixed viewing angle, faster rotation induces makes the observed line wider and increases the flux around the line's center.

Garavito-Camargo et al. (2014) presented in the Appendix an analytical model that accounts for these two features. The basic assumption of the analytical model is that each differential surface element on the sphere Doppler shifts the photons that it emits In this paper we introduce this ansatz by post-processing the results of the outflow simulations without rotation. This allows us to produce new Lyα spectra and compare them with the full radiative transfer solution including both outflows and rotation.

3 RESULTS

3.1 Monte-Carlo Radiative Transfer Model

We evaluate first the effects of increasing rotational velocity at fixed values of the optical depth and outflow velocity. Figure 1 summarizes the information. All plots correspond to the same outflow velocity of $v_{\rm out} = 50$km s^{-1}, rows have constant optical depth and columns have constant rotational velocity. Each panel shows different morphologies corresponding to varying line-of-sight viewing angle.

We now evaluate the effects of increasing outflow velocity at fixed values for the optical depth and rotational velocity. Figure A2 summarizes the information following the same patters as Figure A1, only that this time all plots correspond to the same rotation velocity of $v_{\rm rot} = 50$km s^{-1}.

3.2 Doppler Shifts to Include Rotational Effects

We know that rotation alone does have an impact on the Lyα line morphology and we get the same influence in it that previous works. Together with the outflows, we found that the resulting spectra is equivalent to a non-rotating galaxy with outflows that undergoes a Doppler Shift in velocity, weighted by amount of photons that if rotating would project their escape in $\hat{k}$'s direction. The formulas to calculate this shift are:

$$V' = V + \vec{v}_{\rm rot} \cdot \hat{k} = V + V_{\rm rot}(xk_x - yk_y) \tag{4}$$

where V' is the new Doppler shifted velocity, V is the velocity caused by outflows and $\vec{v}_{\rm rot} = V_{\rm rot}(x\hat{i} - y\hat{j})$.

Figure 3 displays this Doppler shift for four different configurations with a fixed optical depth $\tau_{\rm H}$. In each cell of the grid there is a Lyα spectrum for a galaxy with only outflows and two Lyα spectra for the galaxy with outflows and rotation, one obtained from the radiative transfer and the other by the Doppler shifting of the non-rotating galaxy.

In order to compare the line created with the radiative transfer process that involves the rotation (RT) and the line with only outflows that is Doppler shifted (DS), we calculate three main characteristics for each spectrum. We measure the line's mean velocity, standard deviation and skewness for both RT's and DS's approaches. We plot the results for each value in Figures 4, 5 and 6, respectively for the same $\tau_{\rm H}$ as Figure 3.

This shows that the DS model can reproduce the main characteristics of the RT one. Because of this, we can introduce rotation effects in any spectra without running the radiative transfer simulations, that usually take a significant amount of time and computational resources.

In addition to this, we also evaluate the effects of the viewing angle for fixed rotational and outflows velocity. We measure the intensity of the valley between peaks, for each θ and $\tau_{\rm H}$. Figure 7 summarizes the information with all plots corresponding to the same outflow velocity of $v_{\rm out} = 75$km s^{-1}and rotation velocity of $v_{\rm rot} = 50$km s^{-1}.

4 DISCUSSION
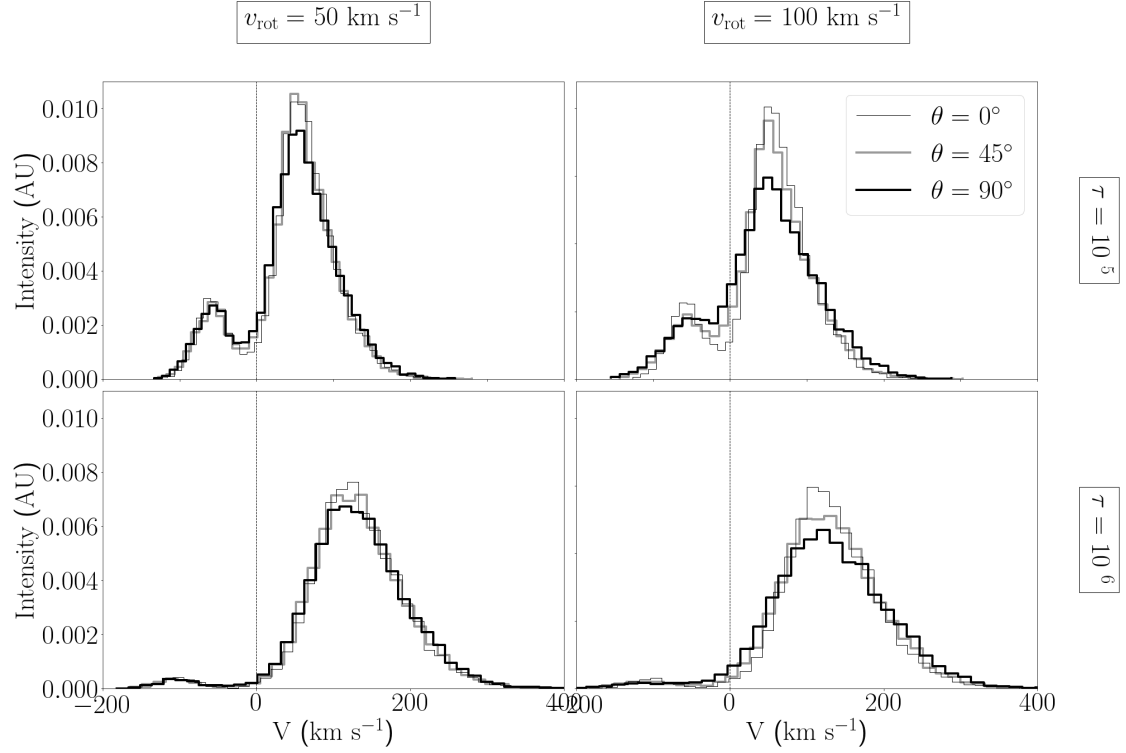
4.1 Theoretical Insights

Talk about radiative transfer...

Figure 1. Spectra for fixed outflow velocity: We fixed $v_{out} = 50$km s^{-1}. We vary v_{rot} increasing from left to right, τ_H increasing from top to bottom, and θ according to the legend.

Regarding de Doppler shift... Then, the quality and accuracy of the spectrum, obtained by a Doppler shift, increases with the optical depth τ_H. This is because the more τ_H, the more anisotropic is the photons' distribution at the galaxy's border.

The introduction of rotation in the model implies that it will only affect galaxies with its viewing angle...

4.2 Application to observational data

Kulas...

MUSE...

5 CONCLUSIONS

APPENDIX A: ADDITIONAL FIGURES

In this appendix we show Figures A1 and A2 with more combinations of v_{rot} and v_{out}.

REFERENCES

Ahn S.-H., Lee H.-W., Lee H. M., 2003, MNRAS, 340, 863
Dijkstra M., Haiman Z., Spaans M., 2006, ApJ, 649, 14
Forero-Romero J. E., Yepes G., Gottlöber S., Knollmann S. R., Cuesta A. J., Prada F., 2011, MNRAS, 415, 3666
Garavito-Camargo J. N., Forero-Romero J. E., Dijkstra M., 2014, ApJ, 795, 120
Partridge R. B., Peebles P. J. E., 1967, ApJ, 147, 868
Verhamme A., Schaerer D., Maselli A., 2006, A&A, 460, 397

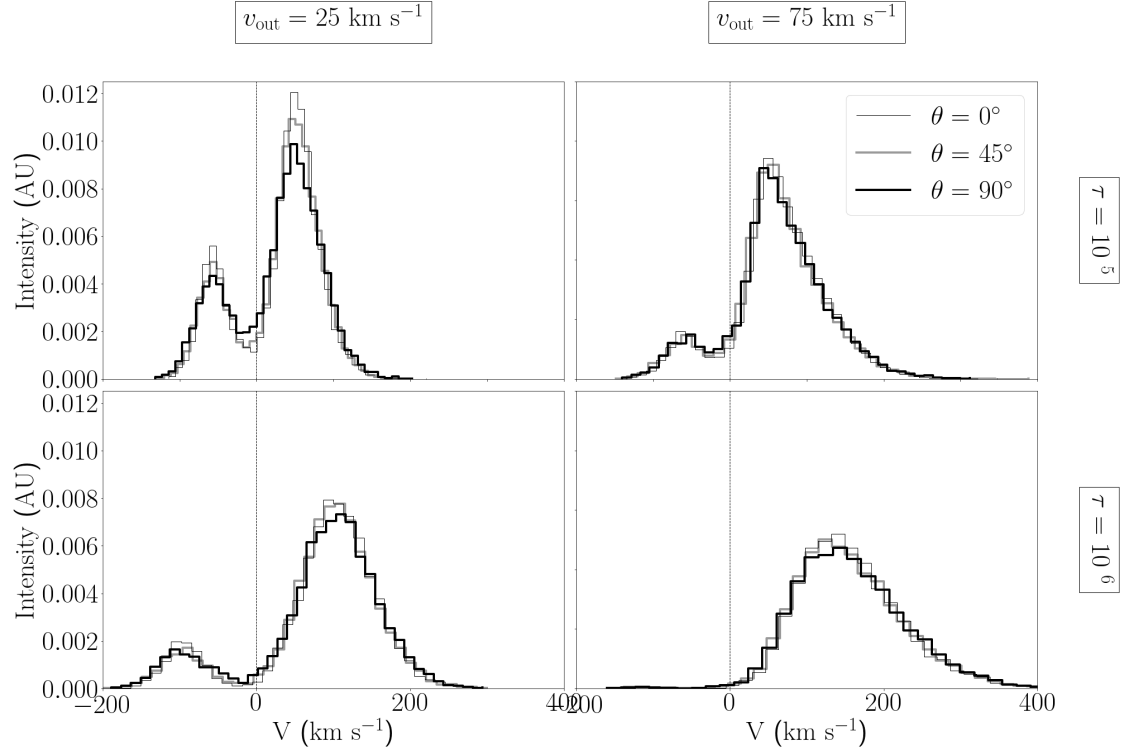**Figure 2. Spectra for fixed rotational velocity:** We fixed $v_{rot} = 50 km s^{-1}$. We vary v_{out} increasing from left to right, τ_H increasing from top to bottom, and θ according to the legend.
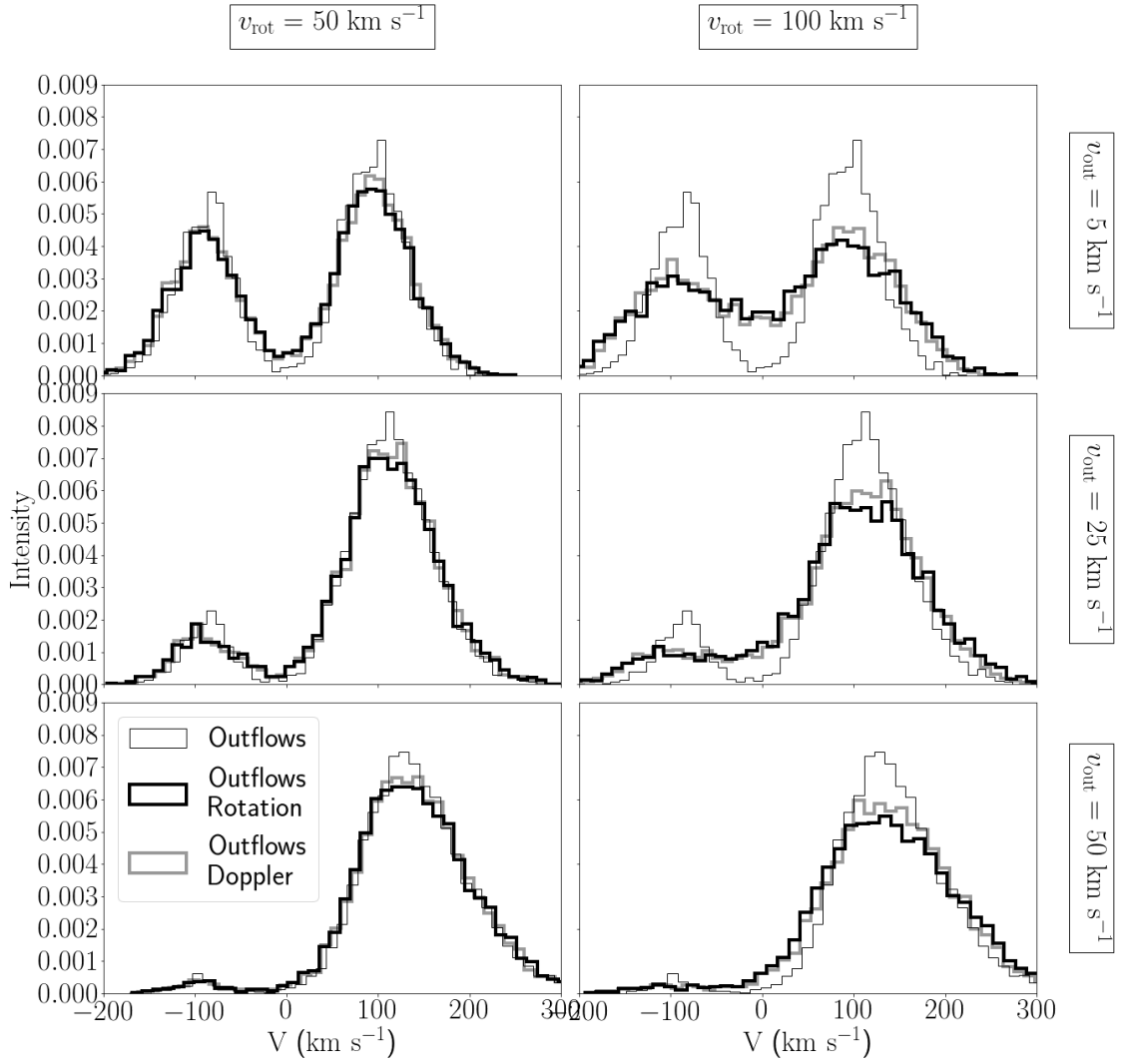
Figure 3. Doppler shift effect: We fixed $\tau_{\rm H} = 10^6$ and $\theta = ?$. We vary $v_{\rm rot}$ increasing from left to right and $v_{\rm out}$ increasing from top to bottom. The legend represents the Lyα line obtained if there is no rotation (in thin line), if there is a radiative transfer of rotation and outflows (thick and clear line), and if there is a radiative transfer of only outflows, but also a Doppler shift from the rotational velocity (thick and dark line).
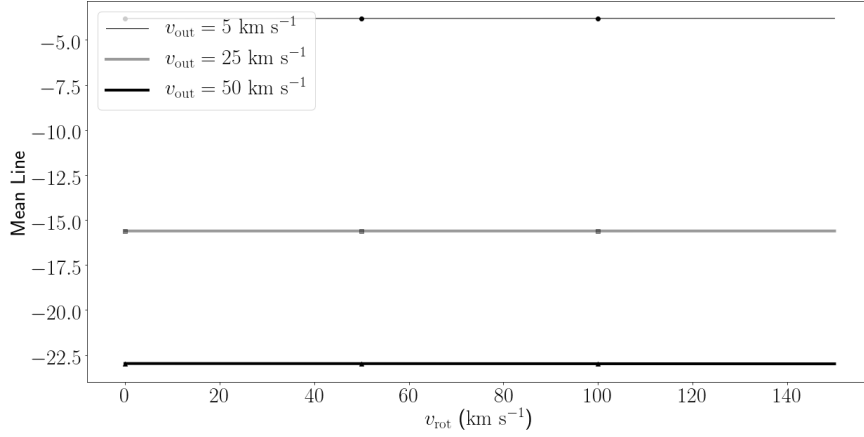
Figure 4. Mean line for RT and DS: The dots represent the Radiative Transfer and the lines represent the Doppler Shift. We fixed $\tau_H = 10^7$.
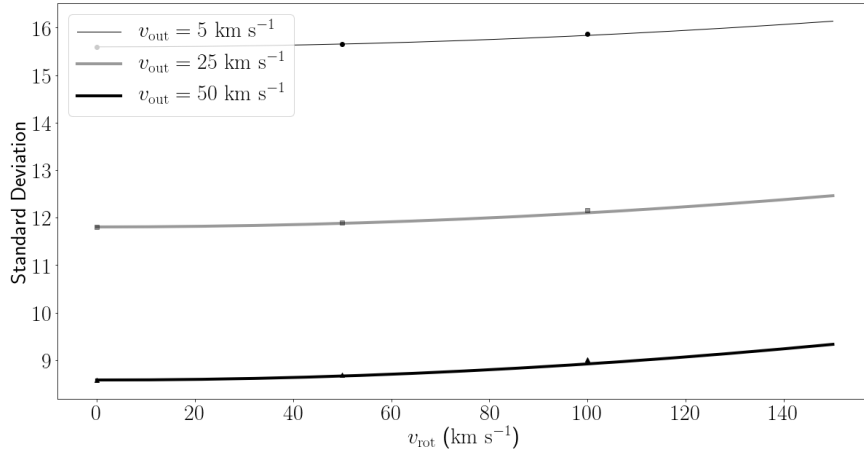
Figure 5. Standard Deviation for RT and DS: The dots represent the Radiative Transfer and the lines represent the Doppler Shift. We fixed $\tau_H = 10^7$.
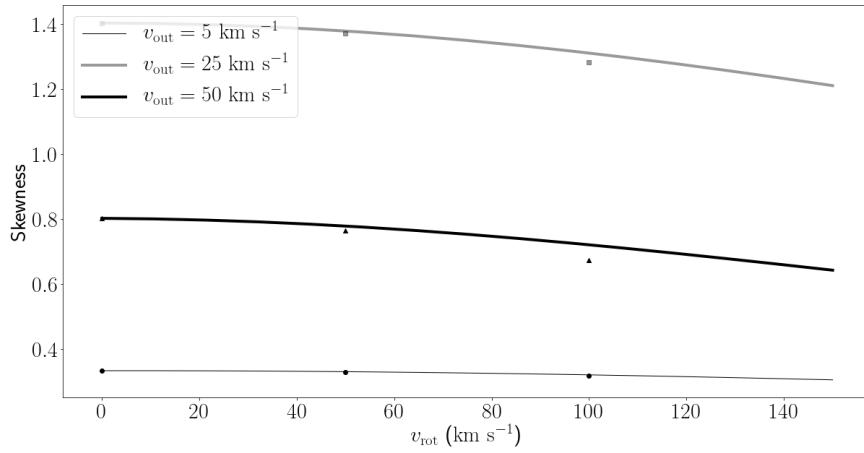

Figure 6. Skewness for RT and DS: The dots represent the Radiative Transfer and the lines represent the Doppler Shift. We fixed $\tau_H = 10^7$.

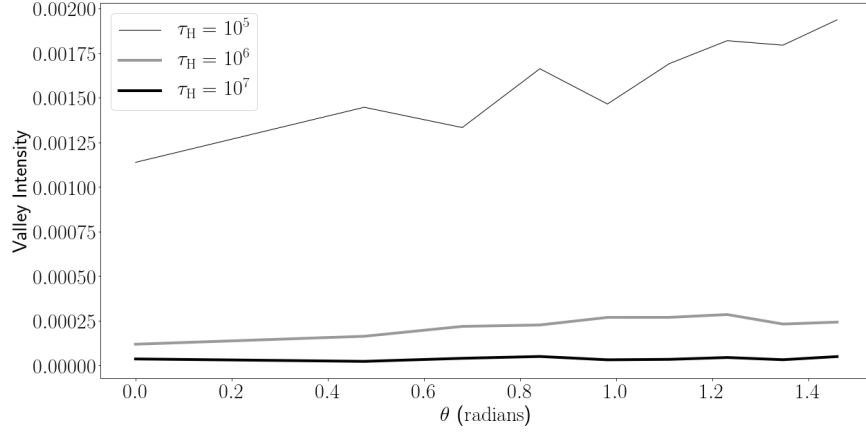**Figure 7. Caption:** We fixed $v_{\text{out}} = 75\text{km s}^{-1}$ and $v_{\text{rot}} = 50\text{km s}^{-1}$.

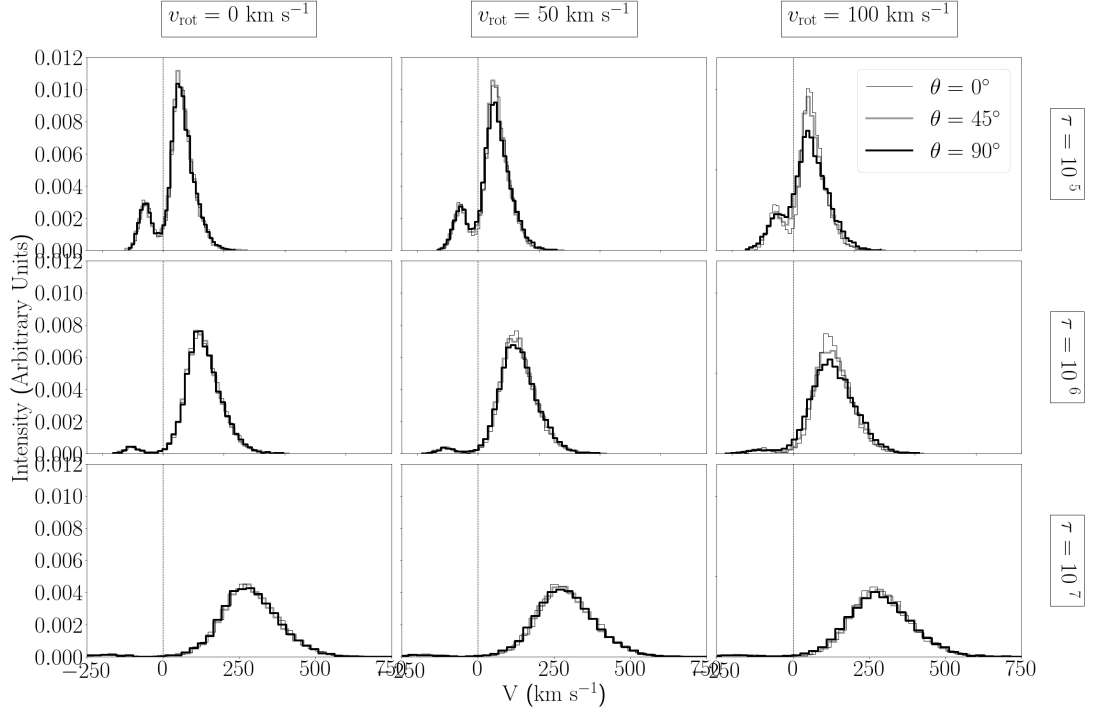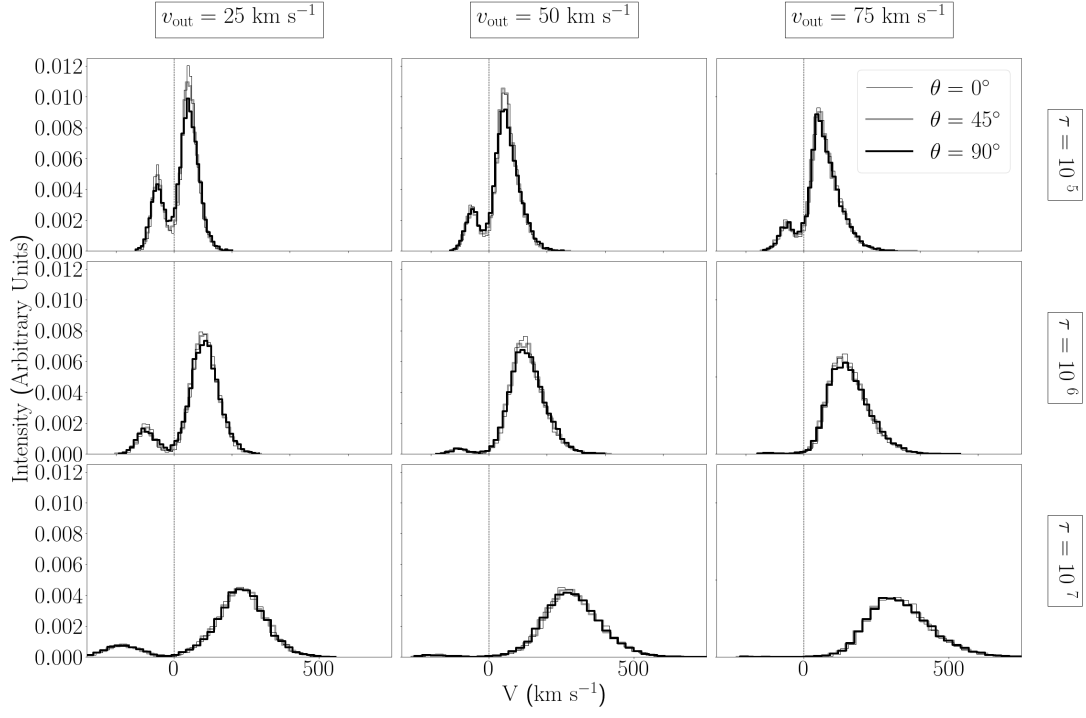**Figure A1. Caption:** $v_{\text{out}} = 50\text{km s}^{-1}$.

Figure A2. Caption: $v_{rot} = 50$km s^{-1}.